Sex differences in IL-17 contribute to chronicity in male versus female urinary tract infection

Anna Zychlinsky Scharff,[1,2] Matthieu Rousseau,[1,2] Livia Lacerda Mariano,[1,2] Tracy Canton,[1,2] Camila Rosat Consiglio,[1,2] Matthew L. Albert,[1,2] Magnus Fontes,[3,4,5] Darragh Duffy,[1,2] and Molly A. Ingersoll[1,2]

[1]Department of Immunology, Institut Pasteur, Paris, France. [2]INSERM U1223, Paris, France. [3]International Group for Data Analysis, Institut Pasteur, Paris, France. [4]The Centre for Mathematical Sciences, Lund University, Lund, Sweden. [5]The Center for Genomic Medicine at Rigshospitalet and Persimune, Copenhagen, Denmark.

Sex-based differences influence incidence and outcome of infectious disease. Women have a significantly greater incidence of urinary tract infection (UTI) than men, yet, conversely, male UTI is more persistent, with greater associated morbidity. Mechanisms underlying these sex-based differences are unknown, in part due to a lack of experimental models. We optimized a model to transurethrally infect male mice and directly compared UTI in both sexes. Although both sexes were initially equally colonized by uropathogenic *E. coli*, only male and testosterone-treated female mice remained chronically infected for up to 4 weeks. Female mice had more robust innate responses, including higher IL-17 expression, and increased γδ T cells and group 3 innate lymphoid cells in the bladder following infection. Accordingly, neutralizing IL-17 abolished resolution in female mice, identifying a cytokine pathway necessary for bacterial clearance. Our findings support the concept that sex-based responses to UTI contribute to impaired innate immunity in males and provide a rationale for non–antibiotic-based immune targeting to improve the response to UTI.

Introduction

Mounting evidence points to the importance of sex in determining susceptibility to infection and immune responses (1–3). For instance, sex-specific differences are evident in bacterial infections by *Legionella, Mycobacterium*, and *Campylobacter* (2). Urinary tract infections (UTIs) exhibit one of the most distinctive sex differences among infectious diseases; adult premenopausal women are 40 times more likely than adult men to experience UTI (4). Consequently, basic and clinical research has overwhelmingly focused on the pathogenesis of UTI in females with little regard for the underlying reasons for this disparity. Importantly, this bias in adult women is not representative of the overall prevalence of UTI in the general population. Indeed, the incidence of UTI is similar between the sexes in infants and the elderly (5). For example, 40% of pediatric UTI patients (<24 months of age) are male (6). Similarly, the incidence of UTI was 14% in women and 11% in men in a healthy geriatric population over the age of 65 (7). These changes in incidence suggest that factors such as sex hormone levels might influence susceptibility to infection during a lifetime (3). Notably, although the incidence of male UTI in adulthood is significantly lower compared with adult women, male UTI patients have an elevated risk of morbidity from complications, as infection in men of all ages is clinically classified as a complicated UTI (8–10). Indeed, although the same first-line antibiotics are used in female and male patients, men require longer treatment durations to eradicate bacteria (11). Together, increased severity and treatment challenges, combined with mounting antibiotic resistance in uropathogenic *E. coli* (UPEC) strains, highlight the need to better understand immunity to UTI in women and men, to determine the mechanisms mediating disease outcome in both sexes. In turn, this knowledge may contribute to the development of non–antibiotic-based stratified therapies targeting sex-specific immune pathways for the treatment of women and men with UTI.

Given the frequency and high morbidity of UTI in infant and elderly males, it is disconcerting that our knowledge of UTI pathogenesis is based almost entirely on studies in female animals. Indeed, transurethral instillation models used to study UTI are performed almost exclusively in female rodents (12–14), and the

technique is broadly reported to be unachievable in male animals (15–19). Only a small number of laboratories report the use of transurethral instillation of bacteria into the male urogenital tract. Studies from these groups investigate prostatitis, and no report has included quantification of bacterial colonization in the bladder or comparison to infected female animals (20–26). To date, only one animal study explored sex differences in UTI, by surgically exposing the bladder abdominally and injecting bacteria through the bladder wall to establish infection (19). The authors observed that male C3H/HeN mice, but not C57BL/6J mice, remain chronically infected following infection (19). Importantly, however, in this model it cannot be excluded that surgery-related inflammation and secondary effects of wound-healing pathways, known to differ between the sexes (27–29), influenced bacterial clearance.

Thus, to test the hypothesis that divergent host responses to UTI between male and female animals results in differential outcomes following infection with UPEC, we established a method of intravesical instillation of bacteria via catheterization of the urethra of male mice (30). This protocol, derived from one routinely used for female UTI studies (12), permitted direct comparison of the innate and adaptive immune response in infected female and male animals over time. C57BL/6J female mice resolved their infection without intervention, as previously reported (31, 32); however, male mice displayed persistent bacteriuria, remaining chronically infected for at least 1 month. Within the first 24 hours following infection, female mice exhibited more robust cytokine expression accompanied by greater immune cell infiltration. Cytokine expression, immune cell infiltration, and resolution were attenuated or abrogated in testosterone-treated female mice. These findings suggest that the increased severity associated with male UTI is due to hormone-mediated suppression of the innate immune response.

Results

Male mice fail to resolve UPEC infection. To directly compare transurethrally infected female and male animals, we adapted a protocol to catheterize female mice to male animals (12). A detailed video protocol of our method is reported elsewhere (30). To investigate the capacity of female and male mice to resolve UPEC infection, we intravesically instilled 7-week-old C57BL/6J mice of both sexes with 1×10^7 colony forming units (CFU) of 1 of 2 isogenic UPEC UTI89 strains bearing resistance to ampicillin (UTI89-GFP-amp^R) or kanamycin (UTI89-RFP-kan^R) (31). Strikingly, we observed that a majority of male mice remained chronically infected up to 1 month, as determined by the presence of UPEC in the urine, in contrast to female mice, which resolved infection (Figure 1A). We sacrificed experimental groups at predetermined time points to quantify bladder bacterial burden. Although female and male mice were equally colonized at 24 and 48 hours postinfection (PI), bacterial burden decreased over time in female mice but remained elevated in male mice, resulting in statistically significantly higher bacterial burdens in male mice 28 days PI (Figure 1B). At 28 days PI, 100% of female mice (21 of 21), but only 29% (7 of 24) of male mice had sterile urine (percentages calculated from animals shown in Figure 1B). Importantly, female mice that resolve an acute infection have no UPEC in their urine but maintain bacterial burdens of approximately 1×10^3 CFU in quiescent tissue reservoirs in C57BL/6J mice (Figure 1B, 28 days PI) (31, 32). In a female UTI model, infection is not confined to the bladder and the kidneys can be colonized by vesicoureteral reflux (33). To determine the extent of infection in male mice, we infected mice with 1×10^7 CFU UTI89-GFP-kan^R and assessed bacterial colonization 60–90 minutes PI. Bacterial CFU in male mice were comparable to CFU previously reported in female mice at the same time point (Supplemental Figure 1A; supplemental material available online with this article; https://doi.org/10.1172/jci.insight.122998DS1) (34). UPEC also colonized the prostate, kidneys, seminal vesicles, preputial glands, and testes in a majority of mice at this time point (Supplemental Figure 1A). Over time, kidney colonization was equivalent between the sexes until 14 days PI, when CFU declined in female mice and increased in male mice (Supplemental Figure 1B). Finally, in male mice, the prostate, seminal vesicles, preputial glands, and testes were colonized for at least 14 days (Supplemental Figure 1C).

Female and male mice mount a nonsterilizing adaptive immune response to UTI. We previously reported that female mice develop a nonsterilizing adaptive immune response following primary UTI that is abrogated in female *Rag2$^{-/-}$* mice (31). Whereas bacterial burden is reduced 2–3 logs in wild-type mice following challenge infection compared with primary UTI, bacterial burden in *Rag2$^{-/-}$* mice is equivalent following primary and challenge infection. Indeed, female *Rag2$^{-/-}$* animals can resolve a primary UTI, suggesting that adaptive immunity is dispensable for bacterial clearance (31). Based on this observation, it was unlikely that a failure to mount an adaptive immune response could explain why chronic infection developed in male
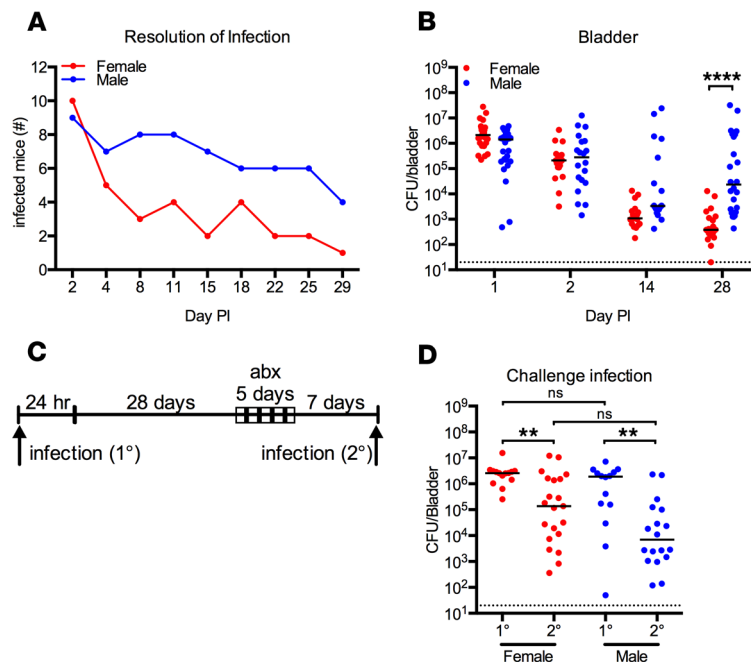
Figure 1. Male mice do not resolve UTI following intravesical instillation. (**A** and **B**) Seven-week-old female and male C57BL/6J mice were infected with 1×10^7 CFU of UPEC strain UTI89-RFP-kan[R] or UTI89-GFP-amp[R]. Graphs depict (**A**) the number of infected mice, determined by urine sampling, and (**B**) CFU/bladder. (**C**) Schematic of the experiment depicted in **D**: female and male C57BL/6J mice were infected with 1×10^7 CFU of UPEC strain UTI89-GFP-amp[R] and bladder bacterial burden was determined 24 hours after primary (1°) infection. At 29 days postinfection (PI), all animals were treated with antibiotics (abx) for 5 days, followed by a 7-day wash-out period. After determination that all mice had sterile urine, mice were challenged with 1×10^7 CFU UPEC strain UTI89-RFP-kan[R] and CFU in bladders determined at 24 hours after challenge (2°) infection. (**D**) The graph shows bacterial CFU at 24 hours after primary or challenge infection in the bladder. **A** depicts representative data ($n = 10$ female, $n = 9$ male) from 1 of more than 5 experiments; red is female, blue is male. Data in **B** and **D** are pooled from 2–4 experiments, $n = 6$–10 mice/group in each experiment. Each dot represents 1 mouse, red denotes female mice and blue indicates male mice, and lines are medians. Dotted lines depict the limit of detection of the assay, 20 CFU/bladder. In **B**, ****$P < 0.0001$, Kruskal-Wallis test comparing female to male at each time point, with Dunn's post hoc test to correct for multiple comparisons. In **D**, **$P < 0.01$, ns = not significant, Kruskal-Wallis test comparing 1° with 2° infection within a single sex and comparing 1° or 2° CFU between sexes, with Dunn's post hoc test to correct for multiple comparisons.

mice. To experimentally rule out this possibility, we employed a model of challenge infection (Figure 1C) (31). Female and male mice were infected with 1×10^7 CFU of UTI89-GFP-amp[R] and a cohort of each sex was sacrificed at 24 hours PI. Although 20 of 21 female animals had sterile urine, compared with only 3 of 18 male mice, we treated both sexes beginning at 29 days PI with trimethoprime-sulfamethoxazole (TMP-SMX, Avemix) in the drinking water, to control for potential influence of antibiotic treatment (Figure 1C). Following a 5-day antibiotic treatment and a subsequent 7-day wash-out period, mice were confirmed to have sterile urine and then infected with the isogenic UPEC strain, UTI89-RFP-kan[R]. Comparable to that observed in Figure 1B, bacterial burden was not different between female and male mice 24 hours after primary infection (Figure 1D). As we previously reported, bacterial burden was significantly lower in female mice 24 hours after challenge infection compared with primary infection, and as hypothesized, bacterial burden was also significantly reduced in male mice following challenge infection (Figure 1D). Bacterial burden in challenged animals was not statistically significantly different between the sexes, suggesting that both female and male mice mount an adaptive immune response capable of reducing but not eliminating bacterial burden following a challenge infection.

Female mice exhibit greater cytokine responses to UTI than male mice. The results of our challenge infection experiments ruled out the possibility that a weak or absent adaptive immune response accounted for differences in resolution of UTI between the sexes. In addition, as female *Rag2*−/− mice, lacking T and B cells, or T cell–depleted mice resolve primary infection with the same kinetics as wild-type female mice (31), we reasoned that the failure to resolve infection in male mice was due to differences in an innate mechanism. To identify innate host factors contributing to resolution in female mice or chronic infection

Table 1. Analytes defining the response to infection, compared with PBS instillation, at 24 hours

Analyte	PBS vs. UTI Female mice[A,B]		PBS vs. UTI Male mice[C]		PBS vs. UTI Both sexes[D]	
	P value	*q* value	*P* value	*q* value	*P* value	*q* value
LIF	3.17×10^{-12}	8.25×10^{-11}	2.51×10^{-5}	6.52×10^{-4}	6.82×10^{-17}	1.77×10^{-15}
CXCL1	7.26×10^{-11}	9.44×10^{-10}	1.25×10^{-2}	4.64×10^{-2}	4.63×10^{-12}	3.01×10^{-11}
IL-17	1.13×10^{-10}	9.79×10^{-10}	2.81×10^{-3}	1.46×10^{-2}	1.80×10^{-12}	1.56×10^{-11}
IL-6	7.79×10^{-10}	5.06×10^{-9}	1.38×10^{-4}	1.79×10^{-3}	7.68×10^{-14}	9.98×10^{-13}
CSF1	3.13×10^{-9}	1.63×10^{-8}			7.94×10^{-11}	3.44×10^{-10}
CCL2	3.97×10^{-8}	1.72×10^{-7}	2.19×10^{-4}	1.90×10^{-3}	3.16×10^{-11}	1.64×10^{-10}
CCL11	5.06×10^{-7}	1.88×10^{-6}			6.65×10^{-7}	1.73×10^{-6}
CSF3	1.07×10^{-6}	3.49×10^{-6}	6.35×10^{-4}	4.13×10^{-3}	1.73×10^{-8}	6.41×10^{-8}
CXCL10	2.56×10^{-6}	7.38×10^{-6}			7.76×10^{-5}	1.44×10^{-4}
VEGF	6.51×10^{-6}	1.69×10^{-5}			1.44×10^{-2}	1.79×10^{-2}
IL-1α	2.51×10^{-5}	5.93×10^{-5}			3.18×10^{-4}	4.86×10^{-4}
CXCL9	3.88×10^{-5}	8.41×10^{-5}			6.73×10^{-5}	1.44×10^{-4}
IL-15	6.04×10^{-5}	1.21×10^{-4}			7.51×10^{-5}	1.44×10^{-4}
IL-4	1.02×10^{-4}	1.90×10^{-4}			1.43×10^{-5}	3.39×10^{-5}
IL-2	2.24×10^{-4}	3.89×10^{-4}			2.18×10^{-3}	3.02×10^{-3}
IL-10	6.57×10^{-4}	1.07×10^{-3}			2.21×10^{-3}	3.02×10^{-3}
CCL3	9.38×10^{-4}	1.36×10^{-3}			1.25×10^{-2}	1.63×10^{-2}
IL-1β	8.93×10^{-4}	1.36×10^{-3}	9.90×10^{-3}	4.29×10^{-2}	1.10×10^{-7}	3.58×10^{-7}
CSF2	2.05×10^{-3}	2.80×10^{-3}			1.29×10^{-4}	2.10×10^{-4}
CXCL2	3.34×10^{-3}	4.34×10^{-3}			8.86×10^{-5}	1.54×10^{-4}
IL-13	1.58×10^{-2}	1.96×10^{-2}				
IL-5	2.30×10^{-2}	2.72×10^{-2}			1.87×10^{-7}	5.39×10^{-7}
IFN-γ	3.20×10^{-2}	3.62×10^{-2}				

[A]Values are ordered by decreasing *q* value for analytes that are statistically significantly different between PBS- and UPEC-instilled female mice. *q* values are the FDR-adjusted *P* values. [B]*P* value and *q* value determined by *t* test between PBS-treated and UPEC-infected female mice. [C]*P* value and *q* value determined by *t* test between PBS-treated and UPEC-infected male mice. [D]*P* value and *q* value determined by ANOVA among PBS-treated female mice, UPEC-infected female mice, PBS-treated male mice, and UPEC-infected male mice. The absence of a value indicates that the analyte was not different between PBS and UPEC-infected animals in the group indicated at the top of the column.

in male mice, we assessed cytokine expression at 24 and 48 hours PI, which is the peak of the cytokine response in female mice (34). Female and male mice were instilled with PBS or infected with UPEC strain UTI89-GFP-amp[R] or UTI89-RFP-kan[R] as above, and 32 cytokines were analyzed using Luminex multianalyte analysis on whole bladder tissue homogenates at 24 and 48 hours PI. Twenty-six cytokines were expressed above the minimum detectable concentration plus 2 standard deviations in bladders in at least one condition. Twenty-three out of 26 analytes measured were significantly different (*t* test, false discovery rate–adjusted [FDR-adjusted] *P* value: *q* < 0.05) between PBS-instilled and UPEC-infected female mice at 24 hours PI (Table 1). By contrast, only 7 of 26 analytes were statistically significantly different between control PBS-treated and UPEC-infected male animals (Table 1, *t* test, *q* < 0.05). ANOVA revealed that 21 of 26 analytes were significantly differentially expressed among the 4 groups of PBS-treated and UPEC-infected female and male mice (Table 1, *q* < 0.05). To have a global view of the relative expression pattern of these 21 cytokines in the 4 treatment groups, we used unsupervised hierarchical clustering and found that UPEC-infected females exhibited the highest cytokine expression at 24 hours PI, whereas infected male mice clustered more closely to PBS-treated animals of both sexes than infected female mice (Figure 2A). The absolute protein expression levels of the 23 cytokines listed in Table 1 (PBS vs. UTI female mice) were, overall, greater in infected female animals compared with infected male mice and PBS-treated mice of both sexes at 24 hours PI (Figure 2B). This differential response was short-lived, as female and male mice had, with a few notable exceptions, similar cytokine levels at 48 hours PI, which approached levels comparable to those measured in naive, untreated bladders (Figure 2C). These differences in cytokine expression were unexpected, as bacterial colonization was equivalent at 24 and 48 hours PI between the sexes (Figure 1B).

To determine whether this distinct pattern of cytokine expression might be relevant in the context of human infection, we took advantage of a publically available data set (data set S1 from ref. 35) from
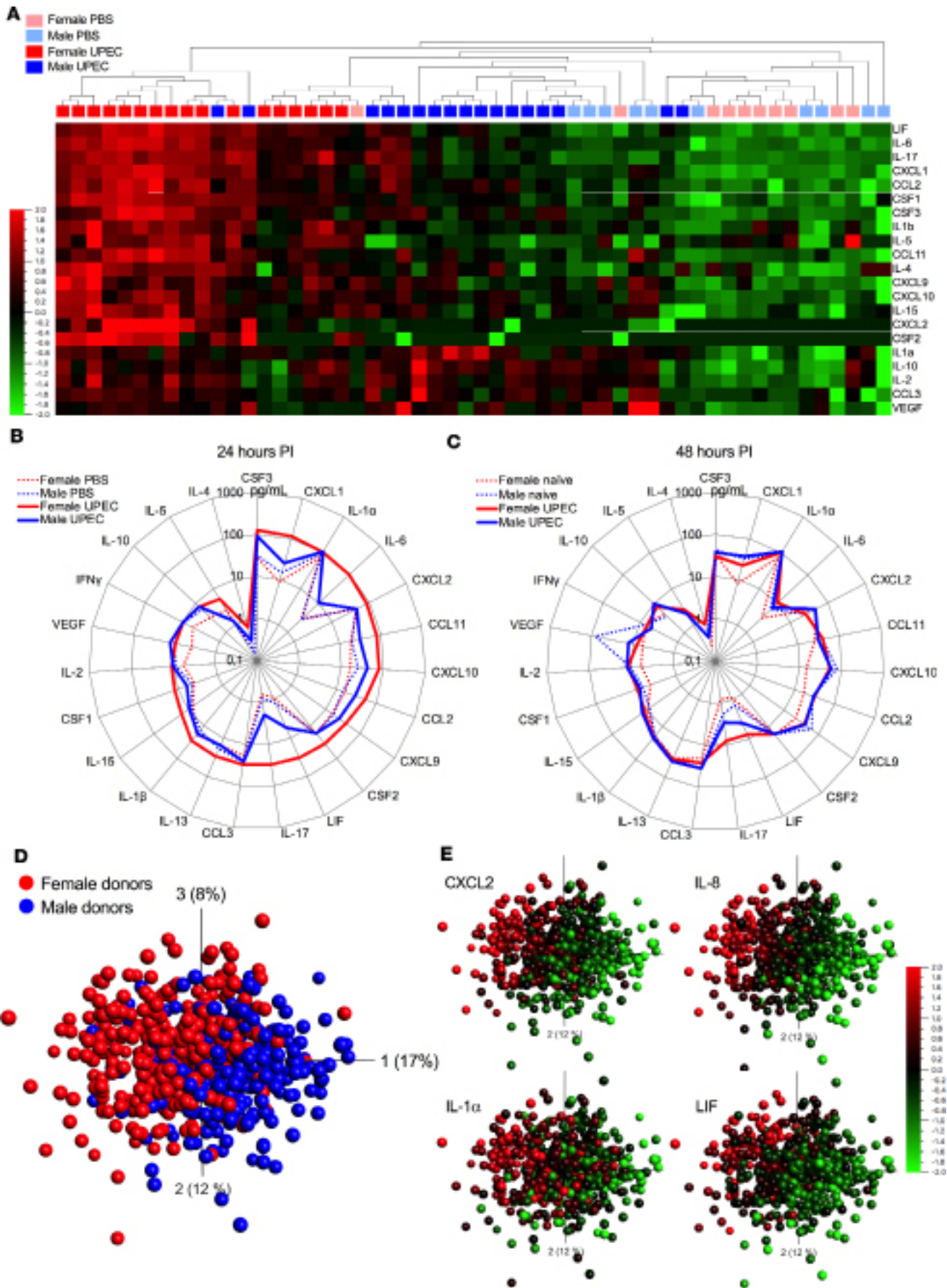
Figure 2. Females exhibit a more robust cytokine response to *E. coli* than males. (**A**–**C**) Female and male mice were instilled with PBS or infected with 1 × 10⁷ CFU of UPEC strain UTI89-RFP-kan^R or UTI89-GFP-amp^R and sacrificed 24 or 48 hours PI. Thirty-two cytokines were measured in homogenized bladders by Luminex assay. (**A**) The heatmap shows unsupervised hierarchical clustering of the 21 significantly different analytes determined by ANOVA (FDR-adjusted *P* value to correct for multiple testing; *q* < 0.05, *P* and *q* values for each cytokine are shown in Table 1) among PBS-treated and UPEC-infected female and male mice. (**B** and **C**) Spider plots show absolute cytokine expression levels (pg/mL) on a log scale at (**B**) 24 hours PI in PBS-treated (dotted lines) and UPEC-infected female (solid red lines) and male (solid blue lines) mice and (**C**) 48 hours PI in both sexes (solid red or blue lines) or in naive, untreated female and male animals (dotted red or blue lines). Data are pooled from 4 experiments, *n* = 5–7 mice per experiment. (**D** and **E**) Analysis was performed on a publically available data set of the transcriptional response in whole blood after stimulation with heat-killed *E. coli* from 300 female and 300 male healthy donors, 20–49 years old. (**D**) The PCA plot represents the variance among 275 genes that are significantly differentially expressed between women (red dots, each dot is a donor) and men (blue dots, each dot is a donor) as determined by ANOVA, *q* < 0.01. (**E**) The mRNA expression level in each donor for *CXCL2*, *IL-8*, *IL-1α*, and *LIF* was overlaid on the PCA plot shown in **D** as a heatmap, in which red represents higher gene expression and green represents lower gene expression.

a recently published study describing the impact of age, sex, and genetics on transcriptional variation in induced human immune responses (35). Using this data set, we investigated differences in gene expression between 300 women and 300 men aged 20–49 (to avoid potential cofounding effects in postmenopausal women), following ex vivo whole blood stimulation with *E. coli*. We observed that 49% (275 of 560) of the immune genes measured showed a significant (*n* = 600, *q* < 0.01) sex association, which can be globally viewed in a principle component analysis (PCA) (Figure 2D; Supplemental Table 1 lists all 275 genes represented in this PCA plot). The expression levels of 4 of these differentially expressed genes, *CXCL2*, *IL-8*, *IL-1α*, and *LIF*, were overlaid on the PCA plot of all differentially expressed genes shown in Figure 2D, illustrating that these cytokines showed higher expression (red color) in female donors and lower expression (green color) in male donors after *E. coli* stimulation (Figure 2E), similar to the pattern observed in mice. Also mirroring our observations in the mouse model, CCL3, IL-4, and IL-1β (Supplemental Table 1), were all significantly (*q* < 0.01) higher in female donors as compared with male donors after stimulation. A sex association with the expression of IL-4R and IL-13R (higher in females), as well as other receptors for cytokines differentially expressed in our mouse model, was also observed (Supplemental Table 1), which would be expected to influence how circulating cells expressing these receptors respond to their cognate cytokines. Together, these findings directly support the potential clinical relevance of our findings in this mouse model.

Immune cell infiltration is greater in infected female mice. Many of the cytokines induced during UTI facilitate the recruitment of innate immune cells to the site of infection (36). To test whether the divergent cytokine response between the sexes impacted immune cell infiltration, we infected female and male mice with UPEC strain UTI89-RFP-kan^R and analyzed bladder tissue by flow cytometry at 24 and 48 hours PI. Infected bladders from female mice had significantly greater numbers of total CD45⁺ immune cells compared with infected male mice (Figure 3A), correlating with increased cytokine expression at 24 hours PI (Figure 2, A and B). Similar to cytokine expression, this difference was evident only at 24 hours PI. While tissue-resident macrophages were not different between the sexes or between naive and infected animals at these early time points, female mice had significantly higher numbers of dendritic cells (DCs) at 24 hours PI (Figure 3B). This increase was modest and did not account for the overall increase in CD45⁺ immune cell populations. By far, the most numerous immune cells were infiltrating neutrophils, monocyte-derived cells, and eosinophils, which were all significantly increased in female mice compared with male mice, only at 24 hours PI (Figure 3C; Supplemental Figure 2, A and B show gating strategy). Differences in immune cell numbers were not due to baseline differences in naive bladder-resident immune cell populations, as flow cytometric analysis of uninfected bladder tissue revealed that the immune cell compartment was not different between female and male mice (Figure 3, A–C; 0 hours PI).

Bacterial uptake is altered in male mice. Previously, we reported that bacteria are found predominantly in resident macrophages at 4 hours PI and are distributed among all phagocytic cells at 24 hours PI in female mice (31). As neutrophils and monocyte-derived cells phagocytose significant numbers of bacteria in female mice (31), we reasoned that the reduced immune cell infiltration in male mice would lead to altered bacterial uptake. To test this hypothesis, we infected female and male mice with UPEC strain UTI89-RFP-kan^R and analyzed bladders by flow cytometry 24 hours PI to assess the identity and the number of phagocytes containing bacteria. To have a global view of UPEC-infected cells, we overlaid traditionally gated populations on a t-distributed stochastic neighbor embedding (tSNE) plot of concatenated infected bladder samples (Figure 4, A and B). We then visualized UPEC-containing immune cells using the same tSNE-generated parameters in female or male bladders, observing that overall, UPEC distribution was sim-
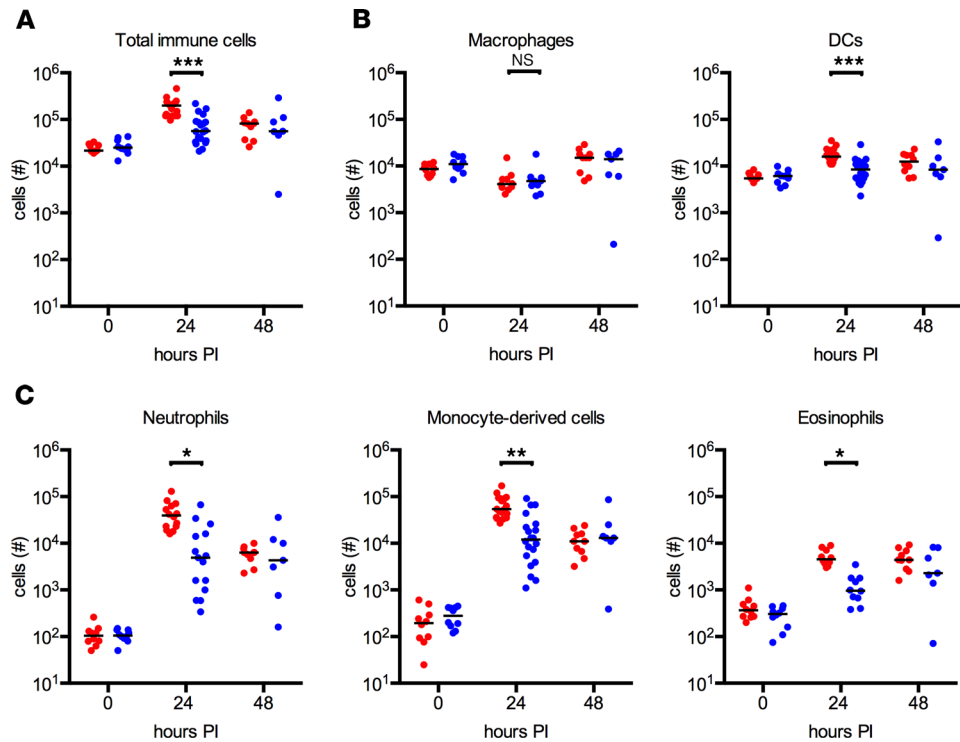
Figure 3. Immune cell infiltration is greater in female mice than male animals following UPEC infection. Female and male mice were infected with 1×10^7 CFU of UPEC UTI89-RFP-kan^R for 24 or 48 hours and bladders analyzed by flow cytometry. Supplemental Figure 2 depicts gating strategies. Graphs depict (**A**) total CD45$^+$ immune cells and (**B** and **C**) total specified immune cell populations at the depicted hours postinfection (PI) in bladders, 0 hours PI = naive mice. Data are pooled from 2–3 experiments, n = 3–7 mice per experiment. Each dot represents 1 mouse, red denotes female mice and blue indicates male mice, and lines are medians. *$P < 0.05$, **$P < 0.01$, ***$P < 0.001$, ns = not significant, Kruskal-Wallis test comparing female to male at each time point, with Dunn's post hoc test to correct for multiple comparisons.

ilar, but female mice had more infected cells compared with male mice (Figure 4C), which was surprising given that similar numbers of UPEC CFU were present in female and male bladder tissue at 24 hours PI (Figure 1B). We quantified the number of infected cells and observed that the majority of UPEC$^+$ immune cells were neutrophils and monocyte-derived cells in both sexes at 24 hours PI (Supplemental Figure 2, C and D show gating strategy; Figure 4D, MHC II$^+$ and MHC II$^-$ monocyte-derived cells are combined in 1 graph). Compared with female mice, however, male animals had fewer UPEC$^+$ monocyte-derived cells, UPEC$^+$ resident macrophages, and UPEC$^+$ DCs at 24 hours PI (Figure 4D). To test whether differences in the number of UPEC$^+$ cells was a result of differential phagocytic capacity between the sexes, we assessed the percentage of UPEC$^+$ cells among defined immune cell populations. While equivalent percentages of neutrophils and monocyte-derived cells contained UPEC in both sexes, female mice had a greater percentage of UPEC$^+$ resident macrophages and DCs compared with male mice, suggesting that the phagocytic capacity of professional APCs may be different between the sexes (Figure 4E).

Testosterone abrogates immunity to UTI in female mice. As hormones are major drivers of sexual dimorphism, we hypothesized that testosterone was responsible for the observed sex difference in bacterial clearance. To specifically test this, we castrated or sham castrated 7-week-old male mice to eliminate the primary source of testosterone, and allowed a 1-week recovery period before infection with UPEC. Resolution of infection was measured by monitoring for the presence of bacteria in urine, and at 28 days PI, bacterial titers were measured in the bladder. We observed no significant differences in bacterial clearance over time or in bacterial burden between mock-treated or castrated mice (Figure 5, A and B), although testosterone levels were efficiently decreased in castrated male mice (Figure 5C).

To address the question of whether estrogen augmentation was needed concurrently with testosterone elimination to resolve infection, we infected male mice that were castrated and then supplemented with slow-release estradiol pellets, and followed bacterial clearance over time. After 28 days of infection, 8 of 12 mock-castrated mice, 5 of 8 castrated/placebo-treated mice, and 4 of 5 castrated/estradiol-supplemented
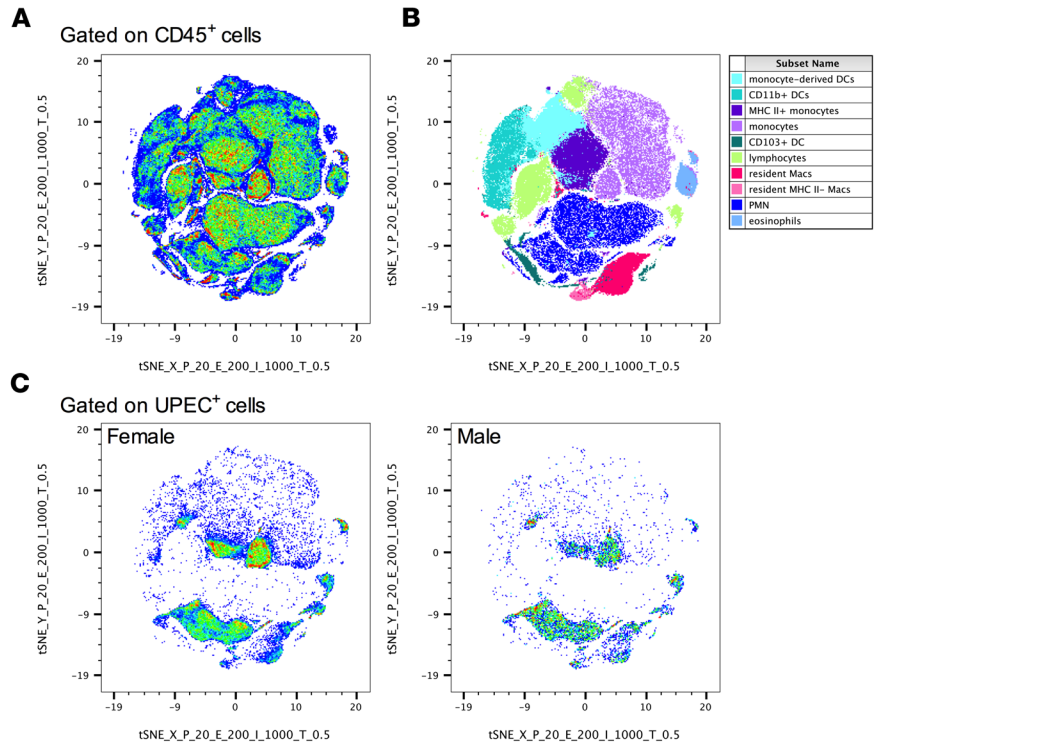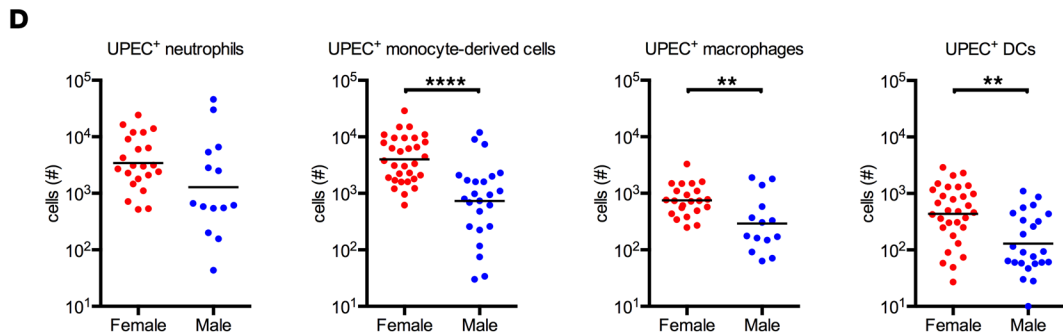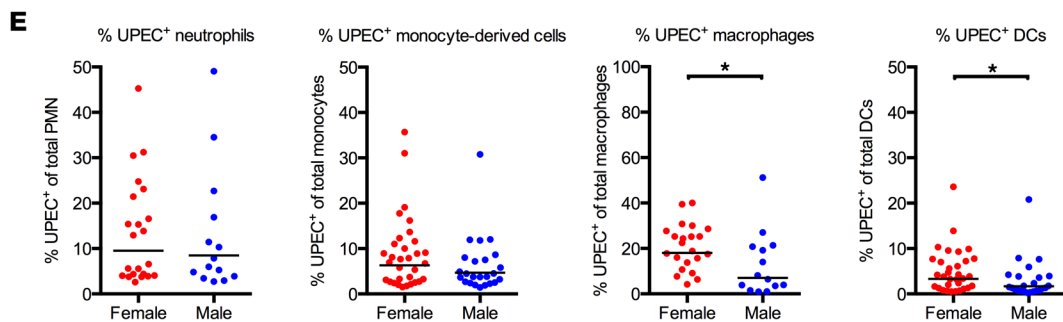
Figure 4. Immune cell populations contain more bacteria in female mice. Female and male C57BL/6J mice were infected with 1×10^7 CFU UPEC strain UTI89-RFP-kan[R] and bladders analyzed by flow cytometry. Supplemental Figure 2 depicts gating strategies. (**A** and **B**) tSNE plots show total CD45+ immune cell populations at 24 hours PI from (**A**) a concatenated sample of 4 female and 4 male mice and (**B**) the same plot with conventionally gated populations overlaid. (**C**) UPEC+ cells from female (left) or male (right) bladders are shown using the same tSNE parameters in **A** and **B**. (**D** and **E**) Graphs show (**D**) the total number of specified immune cell populations containing UPEC and (**E**) the percentage of UPEC+ cells within the specified immune cell populations. Data are pooled from 2–4 experiments, n = 4–5 mice per experiment. Each dot is 1 mouse, red dots depict female mice and blue dots are male mice, and lines are medians. *P < 0.05, **P < 0.01, ****P < 0.0001, Mann-Whitney test. Analyses in this figure were corrected for multiple testing by the Holm–Bonferroni method; all P < 0.05 had q < 0.05.

mice were still infected, demonstrating that estrogen supplementation did not improve the capacity to resolve UTI (Figure 5D). All groups had similar bacterial burdens at 28 days PI (Figure 5E). Complicating interpretation, castration combined with estradiol supplementation resulted in substantial mortality, in which 4 of 12 castrated/estradiol-supplemented mice died prior to or immediately after infection and in the remaining animals, anatomical changes, which only arose in animals supplemented with estradiol, made catheter insertion extraordinarily difficult or impossible, such that 3 of the remaining 8 mice could not be infected.

We next tested the impact of testosterone in female mice using slow-release silastic tubes filled with testosterone or left empty as a control. Animals were permitted to recover 1 week after subcutaneous implantation of tubes before infection with UPEC and bacteriuria was followed over 28 days. Testosterone implantation uniformly elevated plasma testosterone levels in female mice to within the range observed in male mice (Figure 5C). Strikingly, testosterone-treated female mice failed to resolve infection and had persistent bacteriuria for the duration of the experiment, whereas all mock-treated animals had sterile urine by 28 days PI (Figure 5F). Additionally, although testosterone treatment did not alter bacterial burden at 24 hours PI between the 2 groups (Figure 5G), testosterone-treated mice had significantly elevated bladder bacterial burden compared with control mice at 28 days PI, similar to that observed in male mice (Figure 5H). As testosterone can be aromatized to estrogen (37), we measured serum levels of estrogen in testosterone-treated female mice, observing that estrogen levels were not elevated above levels in naive or mock-tube-implanted female mice (Figure 5I). We assessed cytokine expression at 24 hours PI, observing that, similar to infected male mice, testosterone-treated female mice appeared to have lower overall absolute cytokine expression levels compared with control female animals implanted with empty tubing (Figure 5J). Although the lower number of samples ($n = 12$/group) limited the power in this study, statistical analysis and correction for multiple testing revealed that 9 of 26 analytes were significantly differentially expressed ($q < 0.15$, Figure 5K and Table 2) between the 2 groups. CCL11 (eotaxin), was among these cytokines, and accordingly, diminished expression correlated with a decrease in eosinophil infiltration in testosterone-treated mice (Figure 5L). No differences in cellular infiltration were observed for any other cell type between mock-treated and testosterone-treated female mice 24 hours PI (Supplemental Figure 3A). Finally, we were surprised to observe that bacterial uptake, by any cell type, was not altered in persistently infected, testosterone-treated female mice at 24 hours PI (Supplemental Figure 3B), suggesting that chronicity is not directly mediated by reduced phagocytosis early in infection.

Female mice develop an immune response characteristic of type II immunity. IL-4, IL-5, and IL-13 were significantly elevated in female mice compared with male mice during infection and IL-4, IL-9, and IL-13 were more highly expressed in control female mice compared with those treated with testosterone (Figures 2 and 5). In addition, female mice had greater numbers of eosinophils infiltrating infected tissue compared with male mice and testosterone-treated female mice (Figure 5L). Therefore, we hypothesized that female mice initiate a type II immune response mediating resolution of infection that is not induced in male mice. We first tested whether ablation of eosinophils, by administration of anti-SiglecF (α-SiglecF) antibody (38), impacted resolution of infection. Despite reducing the number of circulating eosinophils by 60%–70% (Supplemental Figure 4A), depleting-antibody treatment did not alter the kinetics of resolution in female or male animals over 28 days (Supplemental Figure 4B) or the development of an adaptive immune response (Supplemental Figure 4C).

We then tested upstream mediators of type II immunity. Type II immunity can be initiated by damage to an epithelial cell layer, which is a hallmark of UTI (39). Damage results in the release of alarmins, including TSLP, IL-25, and IL-33, which induce IL-4, IL-5, IL-9, and IL-13 expression, alternative macrophage activation, and innate lymphoid cell (ILC) activation or expansion (40–42). We measured IL-33 and IL-25 expression in bladder tissue finding that, remarkably, IL-33 expression was nearly 3 times higher in female mice compared with male mice at 24 hours PI (Figure 6A). IL-25 was not detected in naive or infected bladder tissue from either sex. Bladder-resident macrophages from female mice upregulated IL-4Rα, which is associated with alternative activation (43), to a greater extent than in male mice during infection (Figure 6B). Additionally, the number of bladder-associated ILCs, defined as CD90$^+$CD3$^-$CD4$^-$NK1.1$^-$MHC II$^-$CD11b$^-$, increased only in female mice 24 hours PI when compared with naive animals (Figure 6C).

We reasoned that exogenous IL-33 would promote resolution of infection in male mice. Male mice were infected and IL-33 was administered directly into the bladder at the time of infection and 24 hours PI (Supplemental Figure 5A). No differences in resolution were observed between the treated and control groups (Supplemental Figure 5B). In addition, IL-33 supplementation did not impact bacterial burden between treated and control animals following primary or challenge infection (Supplemental Figure
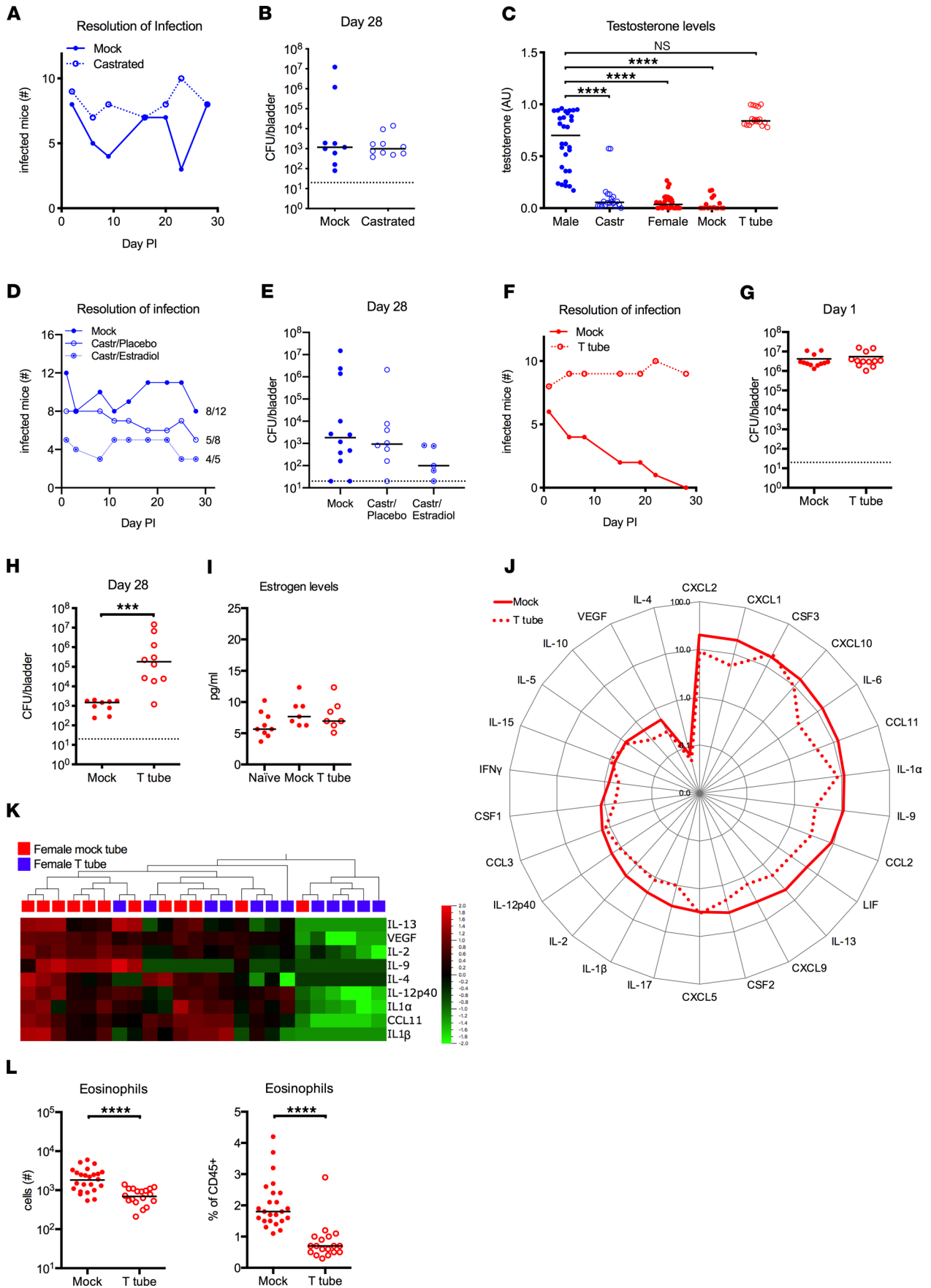
Figure 5. Testosterone treatment induces persistent infection in female mice. (**A–E**) Seven-week-old male C57BL/6J mice were mock castrated (Mock), castrated, or castrated and supplemented with estradiol or placebo pellets and allowed to recover 1 week before infection. (**C** and **F–L**) Female mice were implanted with tubing containing testosterone (T tube) or empty tubing (Mock) and allowed to recover 1 week before infection. All mice were infected with 1 × 10⁷ CFU UPEC strain UTI89-GFP-amp^R or UTI89-RFP-kan^R. Graphs show (**A**) the number of infected male mice over time, (**B**) CFU/bladder 28 days PI in male mice, (**C**) testosterone levels in naive and castrated (Castr) male mice; and naive, empty tube (Mock), and testosterone-treated (T tube) female mice, (**D**) the number of infected male mice over time, (**E**) CFU/bladder 28 days PI in male mice, (**F**) the number of infected female mice over time, (**G**) CFU/bladder 24 hours PI in female mice, (**H**) CFU/bladder 28 days PI in female mice, (**I**) estrogen levels in naive, empty tube (Mock), or testosterone-treated (T tube) female mice. (**J**) Spider plot shows cytokine expression 24 hours PI in mock- and testosterone-treated female mice. (**K**) Heatmap shows unsupervised hierarchical clustering of the 9 significantly different analytes between mock- and testosterone-treated female mice 24 hours PI, analyzed by *t* test, FDR-adjusted *P* value; *q* < 0.15. Analyte *P* and *q* values are presented in Table 2. (**L**) Graphs show the number and percentage of eosinophils in bladders 24 hours PI. See Supplemental Figure 3 for additional immune cell populations. Data are pooled from 2–4 experiments, *n* = 4–10 mice/group in each experiment, except in **A** and **F**, which are a single experiments representative of 2–4 independent experiments. In **B**, **C**, **E**, **G–I**, and **L** each dot is 1 mouse, and lines are medians. In **C**, **H**, and **L**, ***P* < 0.001, *****P* < 0.0001, Mann-Whitney test, FDR *q* = 0.0009 to correct for multiple testing of immune populations analyzed in this figure and accompanying Supplemental Figure 3.

5C). We also tested whether neutralizing IL-33 in female mice would impair bacterial clearance or innate immune responses (Supplemental Figure 5A) (44). Female mice, treated with an α–IL-33 antibody 2 hours prior to infection and 1, 4, and 7 days PI, resolved their infection with similar kinetics and had no differences in bacterial burden following primary or challenge infection compared with isotype-treated mice (Supplemental Figure 5, D and E). At 24 hours PI, treated and control female mice showed no differences in the number of resident immune cells, infiltrating myeloid cells, or lymphocytes as compared with isotype-treated mice (Supplemental Figure 5F). The number of UPEC⁺ immune cells was also not different between the groups (Supplemental Figure 5G). Supporting the idea that type II immune responses were not directly responsible for bacterial clearance, we observed no differences between control and testosterone-treated female mice with respect to IL-33 expression, macrophage IL-4Rα expression, or number of ILCs in infected bladder tissue 24 hours PI (Figure 6, D–F), despite the observation that testosterone treatment abrogated the capacity to resolve infection in female mice.

IL-17 is necessary but not sufficient for resolution of UTI. Having ruled out a role for type II immunity in bacteria clearance, we considered whether other immune cell populations contributed to resolution. In the course of our investigations, we also quantified lymphocytic populations accumulating in the bladder during UTI. We observed that CD3⁺CD4⁺ T cells, NK cells, γδ T cells, and CD4⁺ ILC3 (LTi-like cells, CD90⁺CD25⁺CD4⁺CD3⁻NK1.1⁻MHC II⁻CD11b⁻) were similar in number between naive female and male mice, with the exception of γδ T cells (Figure 7A). These same populations were statistically significantly increased only in infected female mice at 24 hours PI, whereas these cell populations were not different between naive and infected male mice (Figure 7A). Consistent with this observation, these cell populations were decreased in testosterone-treated female mice compared with control-treated mice (Figure 7B). Our previous work ruled out a role for T cells in bacterial clearance (31); therefore, we infected female wild-type and *Rag2⁻/⁻*γc mice, which lack NK cells and ILCs, and followed resolution of infection over time. Remarkably, *Rag2⁻/⁻*γc mice remained infected up to 80 days PI, whereas wild-type female mice resolved their infection within 1 month (Figure 7C). Of note, *Rag2⁻/⁻*γc mice have eosinophils, supporting our conclusion that these cells do not mediate resolution of infection. To specifically test the contribution of NK cells, we infected wild-type female mice treated with a depleting NK1.1 antibody. In contrast to the outcome in infected *Rag2⁻/⁻*γc mice, NK cell depletion did not impact bacterial clearance and both groups of mice cleared their infection by day 28 (Figure 7D).

Our experiments ruled out a role for NK cells in resolution; however, the contribution of ILC3 to UTI immunity was still unclear. Interestingly, *Rag2⁻/⁻* mice can express IL-17 from LTi-like cells (group 3 ILCs or ILC3s) following microbial stimulation, whereas *Rag2⁻/⁻*γc animals do not, as they lack this cell population (45). Of the cytokines expressed in female and male mice during UTI, IL-17 exhibited one of the largest differences between the sexes, which persisted at 48 hours PI (Figure 2, B and C). Thus, we hypothesized that IL-17 expression, early in infection, mediates bacterial clearance. To test whether IL-17 is sufficient for bacterial clearance in male mice, we administered recombinant (r) IL-17 at the time of infection using 2 routes and 2 concentrations, or added additional rIL-17 intraperitoneal injections at 4, 24, and 48 hours PI, and added rIL-17 into the bacterial inoculum (Supplemental Figure 6, A and B). rIL-17 did not impact UPEC colonization at 24 hours PI (Supplemental Figure 6C). We followed infection by monitoring the number of animals with bacteriuria and observed that treatment did not improve the capacity of male mice to resolve UPEC infection in any condition (Supplemental Figure 6, D–F).

Table 2. Analytes defining the response to infection in female mice treated with mock tubes compared to testosterone tubes at 24 hours

	Mock vs. Testosterone tube Female mice[A]	
Analyte	P value	q value
IL-13	2.21×10^{-3}	5.75×10^{-2}
VEGF	7.72×10^{-3}	6.69×10^{-2}
IL-2	5.16×10^{-3}	6.69×10^{-2}
IL-9	1.14×10^{-2}	7.44×10^{-2}
IL-4	1.55×10^{-2}	8.08×10^{-2}
IL-12p40	2.67×10^{-2}	1.07×10^{-1}
IL-1α	3.31×10^{-2}	1.07×10^{-1}
CCL11	3.23×10^{-2}	1.07×10^{-1}
IL-1β	4.12×10^{-2}	1.19×10^{-1}

[A]Values are ordered by decreasing q value for analytes that are statistically significantly different between mock- and testosterone-treated female mice ($q < 0.15$; q values are the FDR-adjusted P values).

Finally, to determine whether IL-17 is necessary for resolution of infection, we administered a single dose of α–IL-17 neutralizing antibody intravenously immediately prior to infecting female mice with 1 of our 2 isogenic UPEC strains and monitored bacteriuria over time. Notably, 8 of 12 mice treated with the α–IL-17 antibody remained infected over 28–35 days, whereas 11 of 12 isotype-treated animals cleared bacteria with the expected kinetics (Figure 7E), supporting the idea that this cytokine is necessary for resolution of UTI; however, in the absence of an inflammatory milieu, such as in male mice, it may not be sufficient to support bacterial clearance.

Discussion

Women experience UTI at a much higher frequency than men, although men develop more severe or chronic infections (9, 10). Anatomical differences between the sexes, such as urethra length, are often proposed as an explanation for the disproportional incidence of UTI in women, despite a lack of experimental evidence to support this hypothesis. Furthermore, this explanation fails to take into account the equivalently high frequency of infection in older men and women (7), and would instead suggest that urethra length changes in aged men, which is not the case (46). Finally, it does not address disparities in the outcome to infection between the sexes (8–10). Hypothesizing that sex-based differences in immunity influence response to UTI, we optimized a model to bypass anatomical differences to directly compare the innate and adaptive immune response in infected female and male mice. Female mice displayed a superior capacity to resolve infection compared with male mice and testosterone-treated female mice. Remarkably, IL-17 neutralization induced chronic infection in female mice. Interestingly, recombinant IL-17 supplementation in male mice was not sufficient to induce bacterial clearance. It is important to note that while 23 of 26 cytokines measured were increased in infected female bladders at 24 hours PI, only 7 were expressed above baseline in infected male bladders, and the magnitude of these changes was less than that of female mice. From these data, we conclude that while IL-17 is clearly necessary for resolution of infection, IL-17 alone is not sufficient to mediate clearance, perhaps due to an insufficiently proinflammatory microenvironment.

IL-17 initiates many antibacterial pathways, including antimicrobial peptide and chemokine expression, recruitment and activation of neutrophils and monocytes, and potentially direct killing of infected cells (47–49). Notably, the majority of the small number of studies reporting IL-17 expression in UTI use pathogens other than UPEC, such as *Proteus* (50, 51), *Streptococcus* (52), *Schistosoma* (53), or *Candida* (54). Furthermore, these studies, as well as those using UPEC (55–57), report changes in IL-17 expression following vaccination or infection, but do not provide evidence that this cytokine supports or regulates host defense or bacterial clearance. Supporting our conclusion that IL-17 contributes to UTI resolution, bladder-associated bacterial CFU are higher in IL-17a^{−/−} mice compared with wild-type animals at 3 and 4 days PI, although whether these mice develop chronic infection is unknown (58). Th17 T cells, γδ T cells, neutrophils, and CD4+ ILC3 can express IL-17 (45, 49). Typically, γδ T cells express high levels of IL-17 following infection or in the context of autoimmune inflammation (49). While γδ T cells are absent
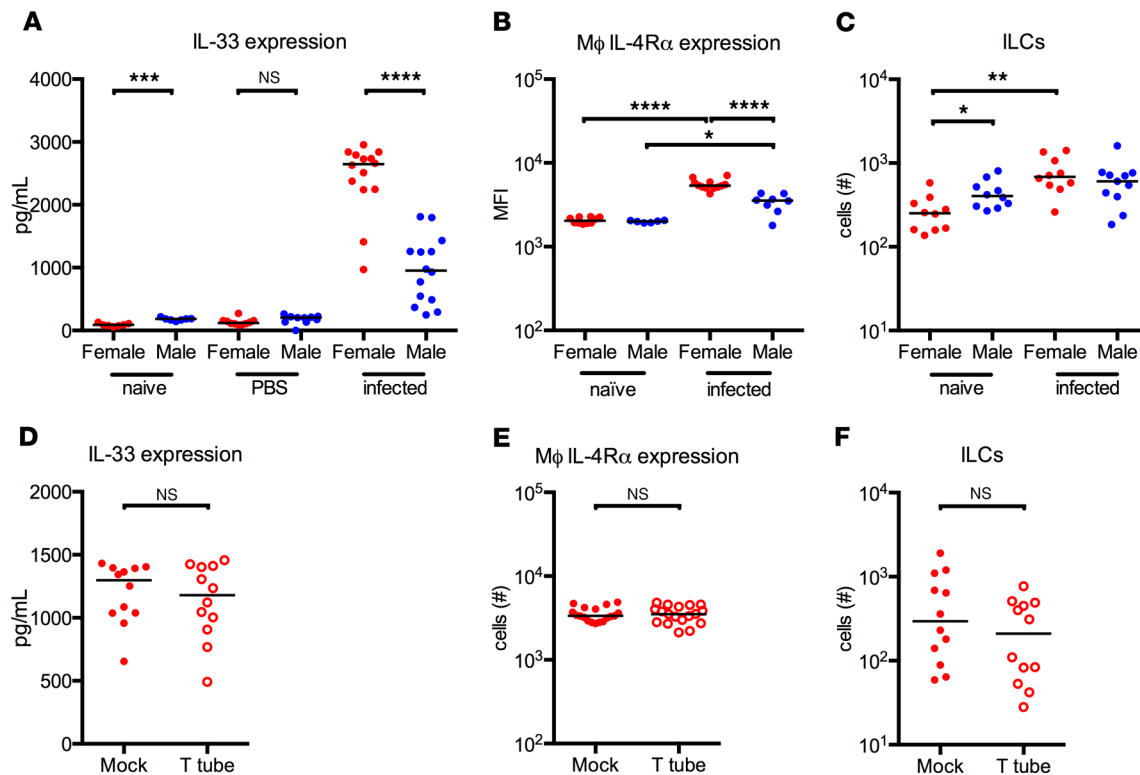
Figure 6. Female mice display characteristics of a type II immune response that is not suppressed by testosterone. (**A–C**) Female and male mice were infected with 1 × 10⁷ CFU of UPEC UTI89-RFP-kanᴿ and bladders analyzed at 24 hours PI. Graphs show (**A**) IL-33 protein levels in homogenized bladder, (**B**) IL-4Rα expression on bladder resident macrophages (Mφ), and (**C**) the number of ILCs (CD90⁺CD3⁻CD4⁻NK1.1⁻MHC II⁻CD11b⁻) in bladders. (**D–F**) Female mice were implanted with empty tubing (Mock) or slow-release tubing containing testosterone (T tube) and allowed to recover 1 week before infection with 1 × 10⁷ CFU UPEC strain UTI89-RFP-kanᴿ. Graphs show (**D**) IL-33 protein levels in homogenized bladder tissue, (**E**) IL-4Rα expression on bladder resident macrophages, and (**F**) the number of ILCs in bladders. Data are pooled from 2–3 experiments, *n* = 4–5 mice/group in each experiment. Each dot is 1 mouse, red dots depict female mice and blue dots are male mice, and lines are medians. ns = not significant, *P < 0.05, **P < 0.01, ***P < 0.001, ****P < 0.0001 by Mann-Whitney test. Analyses in this figure were corrected for multiple testing by the Holm–Bonferroni method; all P < 0.05 had q < 0.05.

in *Rag2⁻/⁻* mice, ILCs are present (45), which may explain why female *Rag2⁻/⁻* mice resolve UTI with wild-type kinetics (31), whereas *Rag2⁻/⁻*γc animals remained chronically infected in this study.

IL-17–mediated inflammation displays sex differences. In an allergic asthma model, male mice exhibit less inflammation compared with female mice and administration of testosterone leads to decreased numbers of IL-17–expressing Th17 T cells and an overall reduction in the level of inflammation associated with lung injury (59). Perhaps, most intriguingly, genetic variation in the Y chromosome imparts varying degrees of protection in a model of flu infection. In this study, infection of Y chromosome consomic C57BL/6J mice revealed that Y chromosome polymorphisms are associated with differences in the frequency of γδ T cells and IL-17 expression, which subsequently impact inflammatory response and disease severity in the lungs (60).

IL-17 may also drive the initiation of pro-resolving type II immunity in the bladder. Indeed, in adipose tissue, the absence of γδ T cells or IL-17 leads to a reduction in IL-33 (61). In this tissue, TNF-α and IL-17 induce upregulation of IL-33, which in turn, controls thermoregulation and response to cold shock (61). Notably, TNF-α is highly expressed in the bladder in the first hour following UPEC infection and, while IL-17 peaks at 24 hours PI, its expression is increased 10- to 100-fold over uninfected female animals 1–6 hours PI (34), potentially inducing the increase in IL-33 observed in this study. Alternatively, we cannot exclude the possibility that differences in IL-33 expression are due to the extent of tissue damage between the sexes; however, this remains to be explored.

The presence of a type II immune signature in UTI was unexpected. Type II immunity is typically associated with parasitic infections and noninfectious inflammatory diseases such as asthma and very few reports have focused on bacterial infection (41, 62, 63). However, the bladder retains metabolic waste until excretion and thus, repair of infected or damaged tissue must occur rapidly. Thus, we speculate that this signaling cascade acts to quickly induce type II immunity pathways to restore the important barrier function
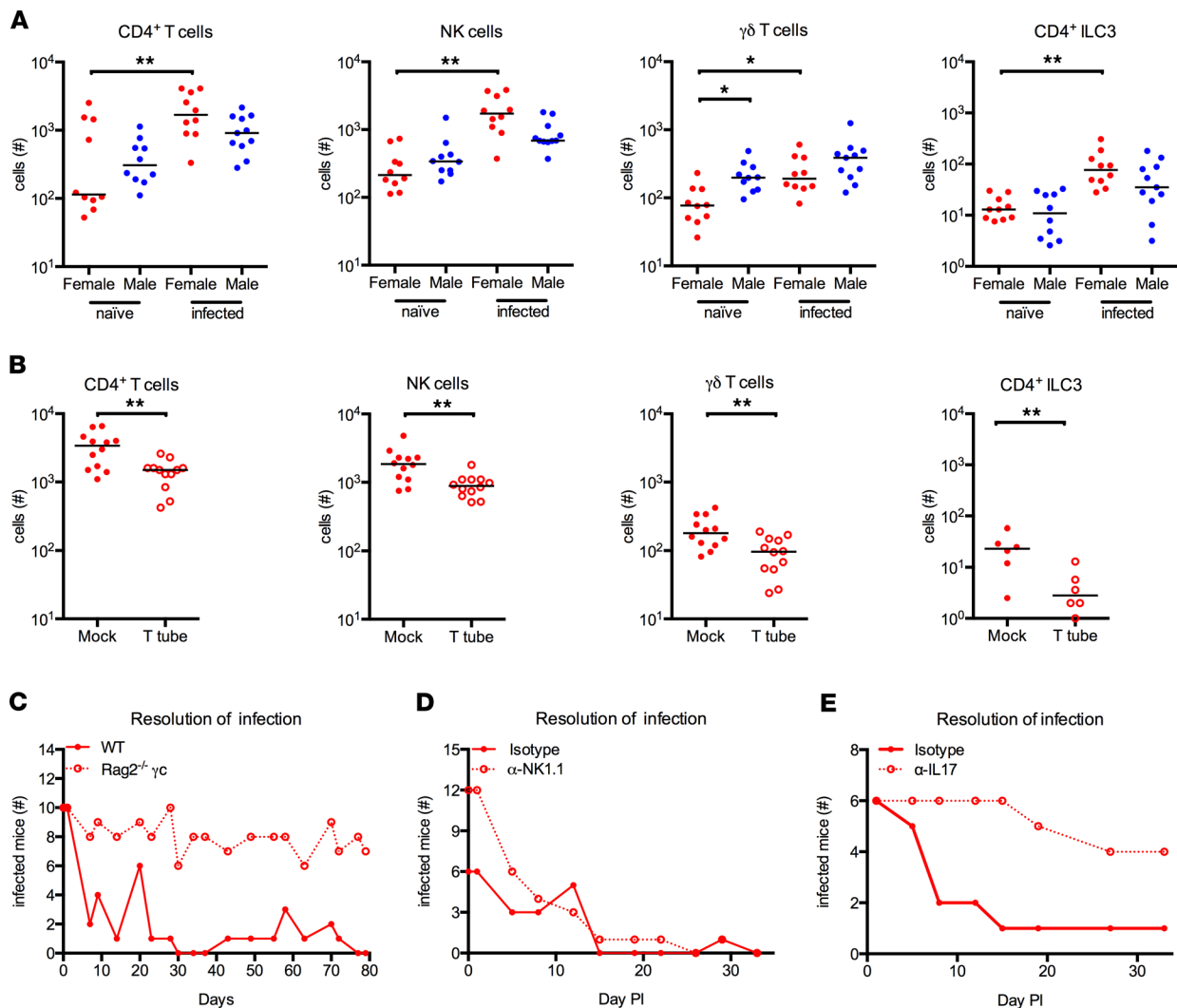
Figure 7. IL-17 is necessary for resolution of infection in female mice. (**A**) Female and male mice were infected with 1 × 10⁷ CFU of UPEC strain UTI89-RFP-kan^R and bladders analyzed by flow cytometry at 24 hours PI. Graphs show (**A**) the number of CD3⁺CD4⁺ T cells, CD3⁻NK1.1⁺ NK cells, γδ T cells, and CD4⁺ ILC3s (CD90⁺CD25⁺CD4⁺CD3⁻NK1.1⁻MHC II⁻CD11b⁻) in bladders. (**B**) Female mice were implanted with empty tubing (Mock) or slow-release tubing containing testosterone (T tube) and allowed to recover 1 week before infection with 1 × 10⁷ CFU UPEC strain UTI89-RFP-kan^R. Graphs show the number of CD3⁺CD4⁺ T cells, CD3⁻NK1.1⁺ NK cells, γδ T cells, and CD4⁺ ILC3s (CD90⁺CD25⁺CD4⁺CD3⁻NK1.1⁻MHC II⁻CD11b⁻) in bladders. (**C–E**) Graphs show the number of infected female mice, determined by urine sampling, over time in (**C**) wild-type or *RAG2⁻/⁻γc* mice, (**D**) mice treated with isotype or NK1.1-depleting antibody, (**E**) mice treated with IL-17–neutralizing antibody. (**A** and **B**) Data are pooled from 2–3 experiments, n = 4–5/group in each experiment. Each dot is 1 mouse, red dots depict female mice and blue dots are male mice, and lines are medians. In **C–E**, graphs are representative experiments, n = 6–12 mice per experiment, 2–3 experiments each. In **A**, *P < 0.05, **P < 0.01 by Kruskal-Wallis test comparing female naive with male naive, female naive with female infected, male naive with male infected, and female infected with male infected, with Dunn's post hoc test to correct for multiple comparisons. In **B**, Mann-Whitney test was used with correction for multiple testing by the Holm–Bonferroni method; all P < 0.05 had q < 0.05.

of the bladder. While this concept remains to be tested, emerging evidence supports the idea that IL-17 and IL-33 work in concert to maintain tissue homeostasis (61).

The cytokine profile observed in female mice suggests that ILCs play a role in the induction of inflammation (ILC3) or reparative functions (ILC2) following infection. Notably, in the lung, ILCs, in female but not male mice, responded to IL-33 treatment by production of large amounts of IL-5 and IL-13, and this cytokine response can be dampened by testosterone treatment (64, 65), suggesting that sex differences in the biology of ILCs influence immunity. This is an exciting new horizon for bladder mucosal immunity as, to the best of our knowledge, bladder-resident ILCs have not been reported. A single publication has described the presence of ILC2 in the urine of patients undergoing bacillus Calmette-Guerin immunotherapy for bladder cancer; however, their origin and function remain unknown (66). Activation and expansion of macrophages and ILCs following IL-33 expression would be expected to induce or amplify expression of

IL-4, -5, -9, and -13, as well as CCL11, mediating eosinophil infiltration (67–69). Thus, eosinophils, while not required for bacterial clearance, likely play a role in another aspect of host defense, repair, or homeostasis. While this is an area that clearly requires further investigation, one possibility is that eosinophils amplify type II immunity supporting development of humoral responses following infection.

What remains to be determined is the underlying cause of this differential cytokine response between female and male mice. Development of chronic UTI in male and testosterone-treated female mice supports the notion that sex hormone levels play an essential role in the response to bacterial colonization. Although we ruled out that testosterone was aromatized to estrogen, and our results in castrated and estradiol-supplemented animals support the idea that testosterone plays a direct role in suppressing the immune response to UPEC infection, estrogen can also play a direct or indirect role in susceptibility to infection, particularly in older patients. Signaling via estrogen receptor α enhances IL-4 and IL-13 expression and polarization of myeloid cells towards an M2-like phenotype (70, 71). Estrogen treatment in vitro increases human β-defensin 3 expression (72), although how this is mediated is unknown. Ovariectomized mice have higher bladder bacterial colonization compared with intact mice (72); however, this was not recapitulated in the surgical model comparing female and male UTI (19). One reason may be that, in addition to the method employed to infect mice (i.e., catheterization of female mice versus incision through the abdominal wall in both sexes), the mouse and bacterial strains differ between these 2 studies (19, 72). Notably, our study utilized one of the same mouse strains and the same bacterial strain as those used in Olsen et al.; however, C57BL/6J mice remained chronically infected only in our study, suggesting that response to surgical manipulation may impact bacterial clearance (19).

In sum, our study demonstrates, in a physiologically relevant model, that IL-17 specifically influences the innate response to bacterial infection in a sex-dependent manner. Interestingly, the first 24 hours of infection were critical in determining whether an animal would resolve infection. Whether the response to infection in this same time period in humans determines outcome remains to be seen; however, our analysis of human samples revealed that a significant number of sex differences in immune gene expression, including players in the IL-17/IL-33 axis, arise in the first 22 hours following *E. coli*–induced immune responses in whole blood. Thus, our work may unlock the potential for fundamental research to better understand immunity in this underappreciated organ, by providing a valuable tool for the investigation of urogenital pathologies that display a sex difference between men and women beyond UTI, such as bladder cancer or interstitial cystitis, and support the development of sex-specific immune modulating therapies to improve the pronounced sex differences observed clinically in response to infection of the urinary tract.

Methods

Study approval. This study was conducted using a preclinical mouse model in controlled laboratory experiments to test the hypothesis that the immune response to urinary tract infection differs between female and male animals. Animals were assigned to groups upon random partition into cages. In all experiments, a minimum of 3 and a maximum of 12 animals made up an experimental group and all experiments were repeated 2–5 times. Data were pooled before statistical analysis and outliers were identified using the Grubbs' test (GraphPad QuickCalcs). In the case of an outlier in a parameter, all parameters measured in the corresponding mouse were excluded. As determined a priori, all animals having abnormal kidneys (atrophied, enlarged, white in color) at the time of sacrifice were excluded from all analyses, as previously we observed that abnormal kidneys negatively impact resolution of infection. Endpoints were determined prior to the start of experiments and researchers were not blinded to experimental groups.

Ethics statement. Animal experiments were conducted in accordance with approval of protocol number 2012-0024 and 2016-0010 by the Comité d'éthique en expérimentation animale Paris Centre et Sud and the Comités d'Ethique pour l'Expérimentation Animale Institut Pasteur (the ethics committee for animal experimentation), in application of the European Directive 2010/63 EU. In all experiments, mice were anesthetized by intraperitoneal injection of 100 mg/kg ketamine and 5 mg/kg xylazine and sacrificed either by cervical dislocation or carbon dioxide inhalation. Human data were from the Milieu Intérieur Project (https://clinicaltrials.gov; identifier: NCT01699893) and were previously described (35). Briefly, publically available data (data set S1: https://www.ncbi.nlm.nih.gov/pmc/articles/PMC5776984/bin/pnas.1714765115.sd01.txt) (35) from 600 healthy volunteers (as defined by inclusion/exclusion criteria) of mainland French origin from the ages of 20–49 years, and stratified by sex were included in our analysis (73).

Mice. Female and male mice between the ages of 5 and 12 weeks were used in this study. C57BL/6J were obtained from Charles River Laboratories France. *RAG2$^{-/-}$γc* were bred in house at Institut Pasteur, Paris.

UTI and determination of bacterial burden. Female and male mice were anesthetized as above, catheterized transurethrally, and infected with 1×10^7 colony forming units of UTI89-GFP-amp[R] or UTI89-RFP-kan[R] (31) in 50 μL PBS as previously described (12, 30). UTI89-GFP-amp[R] and UTI89-RFP-kan[R] infect with equal efficiency (31) and were used interchangeably, with the exception of experiments to detect bacteria by flow cytometry, in which only UTI89-RFP-kan[R] was used because the GFP signal is masked by autofluorescence in the bladder (31).

Infection was monitored by examining bacterial growth from urine samples. Urine was collected every 2–5 days and 2 μL was diluted directly into 8 μL PBS spotted on agar plates containing antibiotics as appropriate. The presence of any bacterial growth was counted as positive for infection. The limit of detection (LOD) for this assay is 500 bacteria per mL of urine. Mice were sacrificed at indicated time points, bladders homogenized in sterile PBS, serially diluted, and plated to determine CFU. The LOD for CFU is 20 or 30 bacteria per organ, depending on the number of dilutions plated, and is indicated by a dotted line in graphs. All sterile organs are reported at the LOD.

Flow cytometry. Mice were sacrificed at indicated time points and the bladders removed. Single-cell homogenates were prepared as previously described (30, 31). Briefly, minced bladders were incubated in 0.34 Units/mL Liberase (Roche) diluted in PBS at 37°C for 1 hour, with manual agitation every 15 minutes. Digested tissue was passed through a 100-μm filter (Miltenyi Biotec), washed, blocked with FcBlock (BD Biosciences), and immunostained (Supplemental Table 2). Samples were acquired on a BD Fortessa (BD Biosciences) and analyzed using FlowJo version 10 software.

Luminex MAP analysis. Bladders were removed at 0, 24, and 48 hours PI and placed in 1 mL of cold PBS and homogenized with a handheld tissue grinder on ice or with a PreCellys24 bead mill homogenizer. One hundred microliters was removed to determine CFU and homogenates were clarified by microcentrifugation (17 x *g*, 4°C, 5 minutes) and stored at –20°C until analysis. After thawing, prior to analysis, samples were centrifuged a second time to remove remaining cell debris. All samples were assessed together to avoid inter-assay variability by Millipore Milliplex MAP Mouse Cytokine/Chemokine Magnetic Bead Panel, Premixed 32-Plex, according to the manufacturer's recommendations (Merck Millipore). Cytokines with values less than the minimal detectable concentration +2 standard deviations (MinDC+2SD, manufacturer's recommendations) in both female and male mice at 24 hours PI, the peak of cytokine expression (34), were removed prior to statistical analysis; these were IL-3, IL-7, IL-12p70, MIP1β, RANTES, and TNF-α.

Castration, hormone implantation, and determination of hormone levels. Five- to 7-week-old male C57BL/6J mice were anesthetized and a small incision made in the scrotum. Testes were externalized, large vessels ligated, and the testes were removed. The incision was closed using VetBond glue. Control (mock) animals received an incision, the testes were exposed, and then the incision was sealed with VetBond. 17β-Estradiol or placebo pellets (0.05 mg/pellet, catalog E-121 or C-111, respectively, Innovative Research of America) were placed under the back skin of mice 1 week after castration by trochar. Empty control and testosterone-filled implants were made according to Ketterson et al. (74). Briefly, silastic tubing (Dow Corning) containing 5 mM packed testosterone propionate (Sigma-Aldrich, catalog 86541), approximately 0.8–1 mg, was implanted under the skin of 6- to 7-week-old female C57BL/6J mice through a small incision. Incisions were closed using 1 or 2 stitches with Vicryl sutures. Control (mock) animals received empty tubing. All mice were allowed to recover for 1 week after each manipulation. Plasma testosterone and estrogen levels were determined by ELISA following the manufacturer's instructions (ab108666 and ab108667, respectively, Abcam).

Cell depletion, recombinant protein supplementation, and protein neutralization. Cell depletion and cytokine neutralization were performed as follows. For SiglecF depletion, 10 μg/mouse α-SiglecF antibody (clone E50-2440, BD Pharmingen) or 10 μg/mouse IgG2a isotype control (clone R35-95, BD Pharmingen) was delivered intraperitoneally in 100 μL PBS (38) at the time of infection, and every 7 days for 3 weeks. For NK cell depletion, 100 μg/mouse α-NK1.1 (clone PK136, BioXCell) or 100 μg/mouse IgG2a isotype control (clone C1.18.4, BioXCell) was delivered intraperitoneally in 100 μL PBS. Mice received isotype control or depleting α-NK1.1 24 hours prior to primary infection and then again on day 6, 13, and 20 after primary infection. For IL-33 neutralization, 3.6 μg/mouse α–IL-33 (catalog number AF3626, BioTechne/R&D Systems) or 3.6 μg/mouse polyclonal goat IgG isotype control (catalog number AB-108-C, BioTechne/R&D Systems) was delivered intraperitoneally in 100 μL PBS (44). Mice received isotype control or neutralizing α–IL-33 two hours prior to primary infection and then again on day 1, 4, and 7 after primary infection. For IL-33 supplementation, mice received 2.5 ng recombinant IL-33 (equivalent to that measured in female mice at 24 hours PI) (catalog number 3626-ML-010, BioTechne/R&D Systems) intravesically at the time

of infection and 24 hours PI. For IL-17 supplementation, mice received 100 pg or 100 ng rIL-17 (catalog number 421-ML, BioTechne/R&D Systems) intravesically or intraperitoneally at the time of infection, or mice received 100 ng intraperitoneally at the time of infection, and 4, 24, and 48 hours PI. In this second experimental design, rIL-17 was also included in the bacterial inoculum at 100 ng/mL. For IL-17 neutralization, 83.3–111 μg/mouse α–IL-17 (clone 50104, BioTechne/R&D Systems) or 83.3–111 μg/mouse rat IgG2a isotype control (clone 54447, BioTechne/R&D Systems) was delivered intravenously in 100 μL PBS. Mice received a single injection of isotype control or neutralizing α–IL-17 at the time of infection.

Statistics. Statistical significance was performed in GraphPad Prism 6 or Prism 8 for Mac OS X using the nonparametric Mann-Whitney test (2 groups) or the nonparametric Kruskal-Wallis test with Dunn's multiple-comparisons post hoc test (3 or more groups) for all data except cytokine analysis and human mRNA expression data. A *P* value of less than 0.05 was considered significant. Multiple testing correction (*q*) within analyses was performed using the Holm-Bonferroni method (https://jboussier.shinyapps.io/MultipleTesting/). Qlucore Omics Explorer 3.2 software was used to test statistical significance of cytokine protein expression data and human mRNA expression data after log transformation of the raw data and to calculate *q* values (the FDR-adjusted *P* value) after log transformation of the values, using either a *t* test or ANOVA as indicated.

Author contributions

AZS, MR, LLM, and MAI conceptualized the study. AZS, MF, and MAI developed the experimental methods. AZS, MR, LLM, TC, CRC, DD, and MAI performed the investigations and data analyses. AZS and MAI wrote the original draft of the manuscript. AZS, MR, LLM, TC, CRC, MLA, MF, DD, and MAI reviewed and edited the manuscript. MLA and MAI acquired funding. MAI supervised the study. AZS and MR contributed equally to this work. AZS initiated the study and MR completed the work. This determined the authorship order.

Acknowledgments

Address correspondence to: Molly A. Ingersoll, Institut Pasteur, 25 Rue du Dr Roux, 75015 Paris, France. Phone: 33.1.45.68.80.71; Email: molly.ingersoll@pasteur.fr.

MLA's and MF's present address is: Department of Cancer Immunology, Genentech Inc, South San Francisco, California, USA.

1. Klein SL, Flanagan KL. Sex differences in immune responses. *Nat Rev Immunol.* 2016;16(10):626–638.
2. vom Steeg LG, Klein SL. SeXX matters in infectious disease pathogenesis. *PLoS Pathog.* 2016;12(2):e1005374.
3. Ingersoll MA. Sex differences shape the response to infectious diseases. *PLoS Pathog.* 2017;13(12):e1006688.
4. Foxman B. The epidemiology of urinary tract infection. *Nat Rev Urol.* 2010;7(12):653–660.
5. Harper M, Fowlis G. 3. Management of urinary tract infections in men. *Trends in Urology, Gynaecology & Sexual Health.* 2007;12(1):30–35.
6. Craig JC, et al. Antibiotic prophylaxis and recurrent urinary tract infection in children. *N Engl J Med.* 2009;361(18):1748–1759.
7. Ruben FL, et al. Clinical infections in the noninstitutionalized geriatric age group: methods utilized and incidence of infections. The Pittsburgh Good Health Study. *Am J Epidemiol.* 1995;141(2):145–157.
8. Conway LJ, Carter EJ, Larson EL. Risk factors for nosocomial bacteremia secondary to urinary catheter-associated bacteriuria: a systematic review. *Urol Nurs.* 2015;35(4):191–203.
9. Lipsky BA. Urinary tract infections in men. Epidemiology, pathophysiology, diagnosis, and treatment. *Ann Intern Med.* 1989;110(2):138–150.
10. Fabbian F, et al. Is female gender as harmful as bacteria? analysis of hospital admissions for urinary tract infections in elderly

patients. *J Womens Health (Larchmt)*. 2015;24(7):587–592.

11. Tandan M, Duane S, Cormican M, Murphy AW, Vellinga A. Reconsultation and antimicrobial treatment of urinary tract infection in male and female patients in general practice. *Antibiotics (Basel)*. 2016;5(3):E31.

12. Hung CS, Dodson KW, Hultgren SJ. A murine model of urinary tract infection. *Nat Protoc*. 2009;4(8):1230–1243.

13. Balemans LT, et al. Effects of sequential intravesical administration of mitomycin C and bacillus Calmette-Guérin on the immune response in the guinea pig bladder. *Urol Res*. 1994;22(4):239–245.

14. Bjorling DE, Wang ZY, Bushman W. Models of inflammation of the lower urinary tract. *Neurourol Urodyn*. 2011;30(5):673–682.

15. Oliveira PA, et al. Technical report: Technique of bladder catheterization in female mice and rats for intravesical instillation in models of bladder cancer. *Scand J Lab Anim Sci*. 2009;36(1):5–9.

16. Seager CM, et al. Intravesical delivery of rapamycin suppresses tumorigenesis in a mouse model of progressive bladder cancer. *Cancer Prev Res (Phila)*. 2009;2(12):1008–1014.

17. El Behi M, et al. An essential role for decorin in bladder cancer invasiveness. *EMBO Mol Med*. 2013;5(12):1835–1851.

18. Hagberg L, Engberg I, Freter R, Lam J, Olling S, Svanborg Edén C. Ascending, unobstructed urinary tract infection in mice caused by pyelonephritogenic Escherichia coli of human origin. *Infect Immun*. 1983;40(1):273–283.

19. Olson PD, Hruska KA, Hunstad DA. Androgens enhance male urinary tract infection severity in a new model. *J Am Soc Nephrol*. 2016;27(6):1625–1634.

20. Wong L, Hutson PR, Bushman W. Prostatic inflammation induces fibrosis in a mouse model of chronic bacterial infection. *PLoS One*. 2014;9(6):e100770.

21. Wong L, Hutson PR, Bushman W. Resolution of chronic bacterial-induced prostatic inflammation reverses established fibrosis. *Prostate*. 2015;75(1):23–32.

22. Boehm BJ, Colopy SA, Jerde TJ, Loftus CJ, Bushman W. Acute bacterial inflammation of the mouse prostate. *Prostate*. 2012;72(3):307–317.

23. Elkahwaji JE, Zhong W, Hopkins WJ, Bushman W. Chronic bacterial infection and inflammation incite reactive hyperplasia in a mouse model of chronic prostatitis. *Prostate*. 2007;67(1):14–21.

24. Lee S, Yang G, Bushman W. Prostatic inflammation induces urinary frequency in adult mice. *PLoS One*. 2015;10(2):e0116827.

25. Shinohara DB, et al. A mouse model of chronic prostatic inflammation using a human prostate cancer-derived isolate of Propionibacterium acnes. *Prostate*. 2013;73(9):1007–1015.

26. Simons BW, et al. A human prostatic bacterial isolate alters the prostatic microenvironment and accelerates prostate cancer progression. *J Pathol*. 2015;235(3):478–489.

27. Knipper JA, et al. Interleukin-4 receptor α signaling in myeloid cells controls collagen fibril assembly in skin repair. *Immunity*. 2015;43(4):803–816.

28. Gilliver SC, Ruckshanthi JP, Atkinson SJ, Ashcroft GS. Androgens influence expression of matrix proteins and proteolytic factors during cutaneous wound healing. *Lab Invest*. 2007;87(9):871–881.

29. Emmerson E, Campbell L, Ashcroft GS, Hardman MJ. Unique and synergistic roles for 17beta-estradiol and macrophage migration inhibitory factor during cutaneous wound closure are cell type specific. *Endocrinology*. 2009;150(6):2749–2757.

30. Zychlinsky Scharff A, Albert ML, Ingersoll MA. Urinary tract infection in a small animal model: transurethral catheterization of male and female mice. *J Vis Exp*. 2017;(130):e54432.

31. Mora-Bau G, Platt AM, van Rooijen N, Randolph GJ, Albert ML, Ingersoll MA. Macrophages subvert adaptive immunity to urinary tract infection. *PLoS Pathog*. 2015;11(7):e1005044.

32. Mysorekar IU, Hultgren SJ. Mechanisms of uropathogenic Escherichia coli persistence and eradication from the urinary tract. *Proc Natl Acad Sci USA*. 2006;103(38):14170–14175.

33. Hopkins WJ, Hall JA, Conway BP, Uehling DT. Induction of urinary tract infection by intraurethral inoculation with Escherichia coli: refining the murine model. *J Infect Dis*. 1995;171(2):462–465.

34. Ingersoll MA, Kline KA, Nielsen HV, Hultgren SJ. G-CSF induction early in uropathogenic Escherichia coli infection of the urinary tract modulates host immunity. *Cell Microbiol*. 2008;10(12):2568–2578.

35. Piasecka B, et al. Distinctive roles of age, sex, and genetics in shaping transcriptional variation of human immune responses to microbial challenges. *Proc Natl Acad Sci USA*. 2018;115(3):E488–E497.

36. Hang L, et al. Macrophage inflammatory protein-2 is required for neutrophil passage across the epithelial barrier of the infected urinary tract. *J Immunol*. 1999;162(5):3037–3044.

37. Simpson ER, Davis SR. Minireview: aromatase and the regulation of estrogen biosynthesis--some new perspectives. *Endocrinology*. 2001;142(11):4589–4594.

38. Zimmermann N, et al. Siglec-F antibody administration to mice selectively reduces blood and tissue eosinophils. *Allergy*. 2008;63(9):1156–1163.

39. Mulvey MA, et al. Induction and evasion of host defenses by type 1-piliated uropathogenic Escherichia coli. *Science*. 1998;282(5393):1494–1497.

40. Fort MM, et al. IL-25 induces IL-4, IL-5, and IL-13 and Th2-associated pathologies in vivo. *Immunity*. 2001;15(6):985–995.

41. Divekar R, Kita H. Recent advances in epithelium-derived cytokines (IL-33, IL-25, and thymic stromal lymphopoietin) and allergic inflammation. *Curr Opin Allergy Clin Immunol*. 2015;15(1):98–103.

42. Walker JA, McKenzie AN. Development and function of group 2 innate lymphoid cells. *Curr Opin Immunol*. 2013;25(2):148–155.

43. Gordon S, Martinez FO. Alternative activation of macrophages: mechanism and functions. *Immunity*. 2010;32(5):593–604.

44. Kim YH, et al. Anti-IL-33 antibody has a therapeutic effect in a murine model of allergic rhinitis. *Allergy*. 2012;67(2):183–190.

45. Takatori H, et al. Lymphoid tissue inducer-like cells are an innate source of IL-17 and IL-22. *J Exp Med*. 2009;206(1):35–41.

46. Kohler TS, Yadven M, Manvar A, Liu N, Monga M. The length of the male urethra. *Int Braz J Urol*. 2008;34(4):451–456.

47. Kolls JK, McCray PB, Chan YR. Cytokine-mediated regulation of antimicrobial proteins. *Nat Rev Immunol*. 2008;8(11):829–835.

48. Veldhoen M. Interleukin 17 is a chief orchestrator of immunity. *Nat Immunol*. 2017;18(6):612–621.

49. Papotto PH, Ribot JC, Silva-Santos B. IL-17. *Nat Immunol*. 2017;18(6):604–611.

50. Habibi M, Asadi Karam MR, Bouzari S. Construction and evaluation of the immune protection of a recombinant divalent protein composed of the MrpA from MR/P fimbriae and flagellin of Proteus mirabilis strain against urinary tract infection. *Microb*

Pathog. 2018;117:348–355.

51. Bameri Z, Asadi Karam MR, Habibi M, Ehsani P, Bouzari S. Determination immunogenic property of truncated MrpH.FliC as a vaccine candidate against urinary tract infections caused by Proteus mirabilis. *Microb Pathog*. 2018;114:99–106.

52. Sullivan MJ, Carey AJ, Leclercq SY, Tan CK, Ulett GC. Increased age, but not parity predisposes to higher bacteriuria burdens due to Streptococcus urinary tract infection and influences bladder cytokine responses, which develop independent of tissue bacterial loads. *PLoS One*. 2016;11(12):e0167732.

53. Schmiedel Y, et al. CD4+CD25hiFOXP3+ regulatory T cells and cytokine responses in human schistosomiasis before and after treatment with praziquantel. *PLoS Negl Trop Dis*. 2015;9(8):e0003995.

54. Ahmadikia K, et al. Increased urine interleukin-17 and interleukin-22 levels in patients with candidal urinary tract infection. *Iran J Kidney Dis*. 2018;12(1):33–39.

55. Hu F, et al. Innate immunity of surfactant proteins A and D in urinary tract infection with uropathogenic Escherichia coli. *Innate Immun*. 2016;22(1):9–20.

56. Carey AJ, et al. Uropathogenic Escherichia coli engages CD14-dependent signaling to enable bladder-macrophage-dependent control of acute urinary tract infection. *J Infect Dis*. 2016;213(4):659–668.

57. Quick ML, Wong L, Mukherjee S, Done JD, Schaeffer AJ, Thumbikat P. Th1-Th17 cells contribute to the development of uropathogenic Escherichia coli-induced chronic pelvic pain. *PLoS One*. 2013;8(4):e60987.

58. Sivick KE, Schaller MA, Smith SN, Mobley HL. The innate immune response to uropathogenic Escherichia coli involves IL-17A in a murine model of urinary tract infection. *J Immunol*. 2010;184(4):2065–2075.

59. Fuseini H, et al. Testosterone decreases house dust mite-induced type 2 and IL-17A-mediated airway inflammation. *J Immunol*. 2018;201(7):1843–1854.

60. Krementsov DN, et al. Genetic variation in chromosome Y regulates susceptibility to influenza A virus infection. *Proc Natl Acad Sci USA*. 2017;114(13):3491–3496.

61. Kohlgruber AC, et al. γδ T cells producing interleukin-17A regulate adipose regulatory T cell homeostasis and thermogenesis. *Nat Immunol*. 2018;19(5):464–474.

62. Gieseck RL, Wilson MS, Wynn TA. Type 2 immunity in tissue repair and fibrosis. *Nat Rev Immunol*. 2018;18(1):62–76.

63. Hogan SP, Waddell A, Fulkerson PC. Eosinophils in infection and intestinal immunity. *Curr Opin Gastroenterol*. 2013;29(1):7–14.

64. Warren KJ, et al. Sex differences in activation of lung-related type 2 innate lymphoid cells in experimental asthma. *Ann Allergy Asthma Immunol*. 2017;118(2):233–234.

65. Cephus JY, et al. Testosterone attenuates group 2 innate lymphoid cell-mediated airway inflammation. *Cell Rep*. 2017;21(9):2487–2499.

66. Chevalier MF, et al. ILC2-modulated T cell-to-MDSC balance is associated with bladder cancer recurrence. *J Clin Invest*. 2017;127(8):2916–2929.

67. Heller NM, Gwinn WM, Donnelly RP, Constant SL, Keegan AD. IL-4 engagement of the type I IL-4 receptor complex enhances mouse eosinophil migration to eotaxin-1 in vitro. *PLoS ONE*. 2012;7(6):e39673.

68. Chen L, et al. IL-4 induces differentiation and expansion of Th2 cytokine-producing eosinophils. *J Immunol*. 2004;172(4):2059–2066.

69. Mould AW, Matthaei KI, Young IG, Foster PS. Relationship between interleukin-5 and eotaxin in regulating blood and tissue eosinophilia in mice. *J Clin Invest*. 1997;99(5):1064–1071.

70. Keselman A, Heller N. Estrogen signaling modulates allergic inflammation and contributes to sex differences in asthma. *Front Immunol*. 2015;6:568.

71. Campbell L, et al. Estrogen receptor-alpha promotes alternative macrophage activation during cutaneous repair. *J Invest Dermatol*. 2014;134(9):2447–2457.

72. Lüthje P, et al. Estrogen supports urothelial defense mechanisms. *Sci Transl Med*. 2013;5(190):190ra80.

73. Thomas S, et al. The Milieu Intérieur study - an integrative approach for study of human immunological variance. *Clin Immunol*. 2015;157(2):277–293.

74. Ketterson ED, et al. Testosterone and avian life histories: the effect of experimentally elevated testosterone on corticosterone and body mass in dark-eyed juncos. *Horm Behav*. 1991;25(4):489–503.